# Bipolar Cascade Superluminescent Diodes at the 1.04-$\mu$m Wavelength Regime

Shi-Hao Guol, Jr-Hung Wang, Yu-Huei Wu, Wei Lin, Ying-Jay Yang, Chi-Kuang Sun, Ci-Ling Pan, and Jin-Wei Shi

***Abstract*—In this study, we investigate the performance of GaAs-based bipolar cascade superluminescent diodes with different cavity lengths. The device operates around the important bio-optical therapeutic 1.04-$\mu$m wavelength window. The introduction of tunnel junctions tends to minimize the nonuniform carrier distribution between distinct multiple quantum-wells (QWs), which is a problem in conventional SLDs, whose electroluminescent spectra are governed by the center wavelength of QWs near the p-side. Our devices exhibit nice electrical characteristics of low leakage current and overcome the limitation of nonuniform carrier distribution, thereby presenting a promising prospect for the near infrared white-light sources.**

***Index Terms*—Amplified spontaneous emission, GaAs, superluminescent diodes.**

## I. Introduction

RECENTLY, cascade light-emitters have been attracting a lot of attention with respect to the achievement of high differential quantum efficiency (DQE) [1] and development of multiwavelength emission [2], [3]. There are two approaches for the fabrication of cascade devices: external and internal. The former method is carried out via a linear cascade of cavity segments in external series [1]. The internal method is characterized by the epitaxial stacking of different active-regimes by tunnel junctions (TJs), the so-called bipolar cascade (BC) devices [2]–[4]. BC devices are often considered more attractive than external approaches due to their compactness, because they do not use an external power combiner, and because of their potential for gain spectrum broadening [2], [3]. Furthermore, it is possible to linearly manipulate the required bias voltage of such cascade devices by controlling the number of units in the series [4]. Therefore, we can let the driving voltage of cascade devices match to the constant voltage power supply and minimize the problem of constant current bias, which can induce excess power consumption [4]. In addition, the distribution of injected carriers and the intensity of light-emission among multiple quantum-wells (MQWs) in BC devices can be made more uniform by the carrier recycling mechanism, in which the injected carriers are reused in each stage after each tunneling process [2], [3]. In relation to this, in our previous work [5], we demonstrated a bipolar cascade superluminescent diode (BC-SLD), which operated with a center wavelength of around 1.04 $\mu$m. This wavelength ($\sim$1 $\mu$m) is an important window for the application of optical coherence tomographic [6] systems, in which a broadband, high-power SLD is the key component for improving the system resolution. In this letter, we further discuss the improvement in device performance, including the bandwidths and improved power.

Manuscript received August 20, 2008; revised October 29, 2008. First published January 06, 2009; current version published February 25, 2009. This work was supported by the National Science Council of Taiwan under Grant NSC 97-2120-M-002-010 and Grant NSC-96-2120-M-002-014.

S.-H. Guol is with the Graduate Institute of Photonics and Optoelectronics, National Taiwan University, Taipei 10617, Taiwan (e-mail: g905055@alumni.nthu.edu.tw).

J.-H. Wang and J.-W. Shi are with the Department of Electrical Engineering, National Central University, Taoyuan 320, Taiwan (e-mail: a1091104345@yahoo.com.tw; jwshi@ee.ncu.edu.tw).

Y.-H. Wu and W. Lin are with Land Mark Optoelectronics Corporation, Tainan 71043, Taiwan (e-mail: stevenwu@lmoc.com.tw; lmocwlin@lmoc.com.tw).

Y.-J. Yang is with Electrical Engineering, National Taiwan University, Taipei 10617, Taiwan (e-mail: yjyang@cc.ee.ntu.edu.tw).

C.-K. Sun is with the Graduate Institute of Photonics and Optoelectronics, National Taiwan University, Taipei 10617, Taiwan. He is also with Electrical Engineering, National Taiwan University, Taipei 10617, Taiwan (e-mail: sun@cc.ee.ntu.edu.tw).

C.-L. Pan is with the Department of Photonics, Chiao Tung University, Hsinchu 300, Taiwan (e-mail: clpan@faculty.nctu.edu.tw).

Color versions of one or more of the figures in this letter are available online at http://ieeexplore.ieee.org.

Digital Object Identifier 10.1109/LPT.2008.2011140

## II. Device Structure and Fabrication

Fig. 1(a) shows cross-sectional and top views of the device, as well as (b) an illustration of the band diagram. The epitaxial layers were grown on (100) orientation n-type GaAs substrates by metal–organic chemical vapor deposition. Strained $In_xGa_{1-x}As$–GaAs well/barrier layers, with an overall thickness of 200 nm, serve as the active regions. The layers all have the same indium mole fractions of 0.34 with distinct thicknesses of 22, 35, 54, and 94 nm, corresponding to ground state (GS) emission wavelengths of 950, 1000, 1050, and 1100 nm, respectively. The position of the four QWs, from left to right, is specified in the schematic band diagram shown in Fig. 1(b). The QWs with center wavelengths of 1100 and 1000 nm are chose to be the center of our active region because of the fact that they have high refractive indices, which can enhance the optical confinement factor. In order to minimize the resorption of photons of shorter wavelength by the neighboring longer wavelength QWs, the center wavelengths of neighboring wells must be as close as possible. We thus adopted QWs with center wavelengths of 1050 and 950 nm, for which the neighboring QWs have wavelengths of 1100- and 1000-nm QW, respectively. The two active regions are connected by the heavily doped backward-positioned $n^{++}/p^{++}$ GaAs-based TJs with corresponding doping concentrations of $5\times10^{18}$ cm$^{-3}/5\times10^{19}$ cm$^{-3}$, respectively. These two layers have the same thickness (10 nm). The TJ layer is sandwiched by a pair of $(n: 1\times10^{18}$ cm$^{-3}; p: 5\times10^{18}$ cm$^{-3})$ wider bandgap material $Al_{0.1}Ga_{0.9}As$ layers, which have the same thickness (20 nm). These layers serve as the carrier confinement layers for reducing the leakage current of the device [7]. The

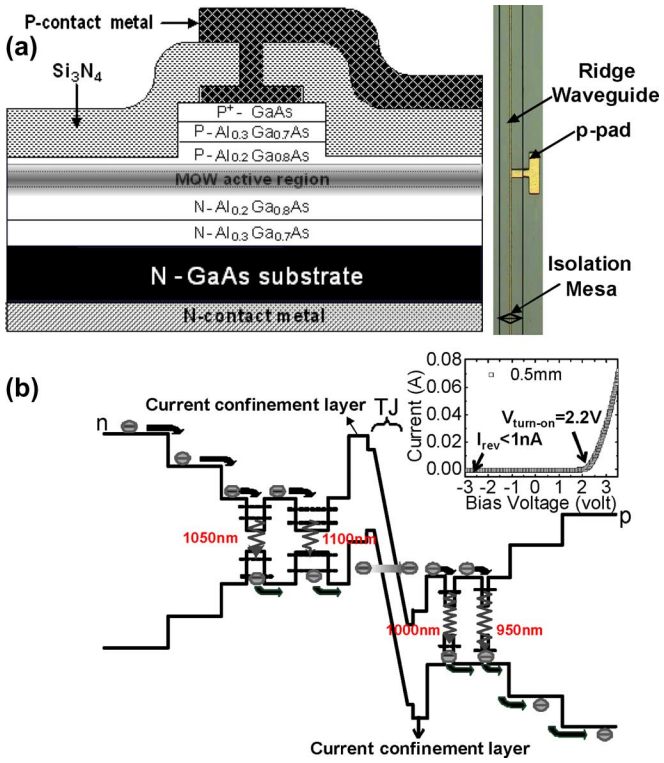


Fig. 1. (a) Cross-sectional and top views of the BC-SLD, as well as (b) schematic band diagram illustrating the device. The inset shows the $I$–$V$ characteristic curve for a cavity length of 0.5 mm under CW operation.

separate confinement heterostructure (SCH) is employed in our device to achieve optical confinement. We add 0.5-$\mu$m-thick $Al_{0.2}Ga_{0.8}As$ core-layers and 0.4-$\mu$m-thick $Al_{0.3}Ga_{0.7}As$ cladding layers around the active regions. In such a structure, where the carrier confinement layers of both $Al_{0.1}Ga_{0.9}As$ and SCH can effectively prevent carriers from directly passing over the TJ thus enhancing the current recycling rate [7]. For device fabrication, dry etching was first utilized to define a straight ridge waveguide (6 $\mu$m wide and 0.8 $\mu$m high), followed by the creation of an isolation mesa by wet etching. Then, the metallization of p-contact metal (Pd–Ti–Pt–Au) and the passivation of $Si_3N_4$ were carried out. After thinning the substrate to $\sim$100 $\mu$m, the metallization of the n-contact and the annealing process were done. Finally, the samples were carefully cleaved into lengths of 0.3, 0.5, and 1 mm. An antireflection coating was deposited on one of the two facets to suppress the lasing phenomenon.

## III. Measurement Results

The demonstrated devices were operated under different continuous-wave (CW) bias or pulse currents at room temperature (RT). The inset to Fig. 1(b) shows the current–voltage ($I$–$V$) characteristics of the 0.5-mm-long BC device during CW operation. The measured differential resistances (10 $\Omega$) are larger than those of the typical GaAs-based SCH QW laser (typically by 3–4 $\Omega$) with a similar geometric size of active area. Such a result can be attributed to the fact that our devices contain two active regions (four QWs) combined by a TJ. The measured 2.2-V turn-on voltage is reasonable due to the fact that the bandgaps of our two cascade regions are both around 1 eV. The $I$–$V$ characteristics of our novel devices differ

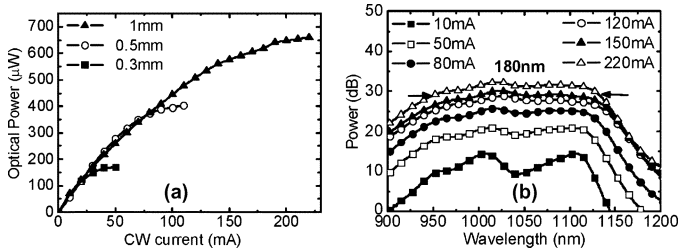


Fig. 2. (a) Free space output optical power measured under different CW bias currents at RT; (b) spectral traces made under different bias currents for the cavity length of 1 mm.

considerably from those reported elsewhere [2], for devices in which large leakage currents can arise under reverse bias operation. This can occur if the backward-positioned $n^{++}/p^{++}$ tunnel diode begins "forward operation" during reverse bias driving. Those devices also exhibit a region of negative differential resistance under forward bias driving. The significant improvement in leakage current ($<$1 nA under $-$3-V operation) in our devices, compared with previous results, can be attributed to the engagement of the carrier confinement layers, as shown in Fig. 1, which minimizes the probability of electrons thermally jumping directly through the TJ. Furthermore, our SCH structure, which can be treated as a diode with a larger bandgap than that of a TJ, successfully blocks the current from the TJ, thus eliminating the existence of negative differential resistance. Fig. 2(a) shows the free space output optical power measured under different CW bias current operations at RT for three different lengths of 0.3, 0.5, and 1 mm. One can clearly see that the optical power can be improved by increasing the cavity lengths. Fig. 2(b) shows the spectral traces obtained under different bias currents for the 1-mm cavity length case. Under low injection current, two peaks appear in the spectrum traces around 1000 and 1100 nm, dominating the electroluminescence (EL) spectra. These wavelengths correspond to the GS emissions of the neighboring MQWs closest to the TJ, as illustrated in Fig. 1(b). As the bias current increases, emissions from the other two QWs gradually take place, and the traces of the optical spectra become flattened to cover all the wavelengths in our design. The full-width at half-maximum (FWHM) optical bandwidth obtained for the 1-mm-long device under a large range of CW bias driving currents (80–220 mA) is from 170 to 180 nm. To the best of our knowledge, there is no other reported GaAs-based light-emitting-diode operating at $\sim$1 $\mu$m with such a large bandwidth [5], [8]. The implication is that the presence of the TJ structure of the TJ in the MQWs acts effectively to increase uniformity of the injected carriers and to successively minimize the problem of nonuniform carrier distribution characteristic of traditional white-light MQW devices [9], whose EL spectrum can be seriously affected by the operating current and by the center wavelength of QWs near the p-side. However, the fact that there is no superluminescent phenomenon under CW current injection can be ascribed to heat problems caused by the larger resistance, as mentioned above. To minimize this problem and to improve the power, we measured the devices using a pulsed current generator under the following conditions: 10-$\mu$s duration and 1/100 duty cycle. Fig. 3(a) shows the free space output power of devices with distinct cavity lengths measured under different pulsed pumping currents at RT. All devices share similar threshold

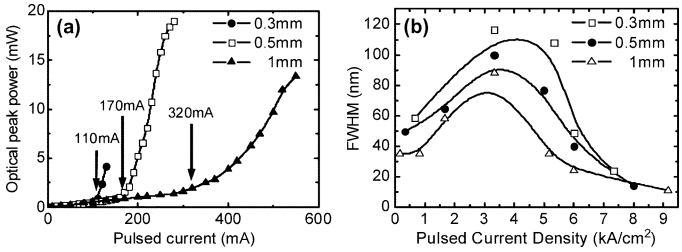


Fig. 3. (a) Measured free space output optical power of distinct cavity length devices under different pulsed current operation at RT; (b) shows the correlation of the measured FWHM optical bandwidths and injected current density.

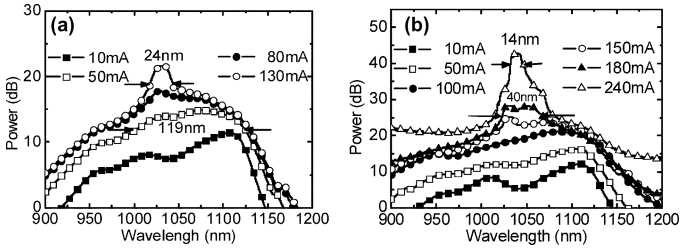


Fig. 4. Spectral traces obtained under different pulsed currents with cavity lengths of (a) 0.3 and (b) 0.5 mm.

current densities of 5.2 kA/cm$^2$ but exhibit different maximum output powers. As can be seen, the 0.3-mm device has the poorest maximum output power performance among the three devices. It failed under a pulse current of only around 130 mA. This may be attributed to the edge-breakdown of the TJ, which was reverse-biased when the device was forward-biased, as well as to heating problems, both of which were most serious in the device with the smallest active area. On the other hand, the 1-mm device suffers from obvious degradation of its DQE, as shown by the slope of curve light output–current ($L$–$I$) in Fig. 3(a). This occurs due to the decrease in DQE with the increase in the active length of the device [10]. The optimal cavity length is 0.5 mm, which exhibits a maximum output power of 19 mW under 280-mA pulsed current operation. Fig. 3(b) shows the FWHMs of the EL spectra of these three devices versus pulse-current density. The device with a shorter cavity length obviously presents a wider FWHM bandwidth under the same injected current density at which point a superluminescent phenomenon occurs (pulse-current density $>$5.2 kA/cm$^2$). This result can be attributed to the higher mirror loss of the short device, which impedes the lasing phenomenon (spectrum narrowing) [11]. For the device with a 0.3-mm active length, the maximized 3-dB bandwidth can be as wide as 119 nm given an output power of 220 $\mu$W under a bias current of 50 mA (3.3 kA/cm$^2$). The corresponding bias dependent optical spectra of the 0.3- and 0.5-mm-long device are shown in Figs. 4(a) and (b), respectively. During low pulsed current injection, all of the demonstrated devices exhibit a hump in the EL spectral traces, similar to the case under CW injection.

For the 0.5-mm device, it can be seen that when the bias current exceeds 100 mA, the 1100-nm GS transition gradually becomes saturated, resulting in flattened EL spectra around 1100 nm, and a peak wavelength of around 1030 nm. From simple calculations, we can identify this emission wavelength as being the result of the first excited state (ES) transition for the 1100-nm wavelength QW. The occurrence of the superluminescent phenomenon at 1030 nm, instead of 950 nm, which is the center wavelength of QW closest to the p-side, once again reveals that our design can overcome the limitation of nonuniform carrier distribution that occurs in traditional SLDs. A 3-dB bandwidth of 40 nm, in which the intensities of the two amplified spontaneous emission maxima become equal, can be acquired for the 0.5-mm-long device driven at 180 mA. Above this, the ES transition becomes superior to all GS ones. The gradually narrowing FWHM bandwidths of these SLDs with the increased current density are presented in Fig. 3(b). We can achieve a maximum peak power of 19 mW with an FWHM bandwidth of 14 nm around the 1.04-$\mu$m wavelength under 280-mA pulsed current pumping, as shown in Fig. 4(b).

## IV. Conclusion

In summary, we studied a new kind of SLD, which utilizes a TJ placed at the center of active region to connect different MQWs. Our demonstrated BC-SLDs present nice electrical characteristics and more uniform distribution of injected carriers among different MQWs.

## References

[1] J. T. Getty, E. J. Skogen, L. A. Johansson, and L. A. Coldren, "CW operation of 1.55- $\mu$m bipolar cascade laser with record differential efficiency, low threshold, and 50-matching," *IEEE Photon. Technol. Lett.*, vol. 15, no. 11, pp. 1513–1515, Nov. 2003.

[2] J. Yan, J. Cai, G. Ru, X. Yu, J. Fan, and F.-S. Choa, "InGaAsP–InP dual-wavelength bipolar cascade lasers," *IEEE Photon. Technol. Lett.*, vol. 18, no. 16, pp. 1777–1779, Aug. 15, 2006.

[3] S. M. Nekorkin, A. A. Biryukov, P. B. Demina, N. N. Semenov, B. N. Zvonkov, V. Y. Aleshkin, A. A. Dubinov, V. I. Gavrilenko, K. V. Maremyanin, S. V. Morozov, A. A. Belyanin, V. V. Kocharovsky, and Vl. V. Kocharovsky, "Nonlinear mode mixing in dual-wavelength semiconductor lasers with tunnel junctions," *Appl. Phys. Lett.*, vol. 90, no. 17, p. 171106, Apr. 2007.

[4] J. P. Prineas, J. T. Olesberg, J. R. Yager, C. Cao, C. Coretsopoulos, and M. H. M. Reddy, "Cascaded active regions in 2.4 $\mu$m GaInAsSb light-emitting diodes for improved current efficiency," *Appl. Phys. Lett.*, vol. 89, p. 211108, Nov. 2006.

[5] S.-H. Guol, J.-H. Wang, Y.-H. Wu, W. Lin, Y.-J. Yang, C.-K. Sun, C.-L. Pan, and J.-W. Shi, "GaAs-based bipolar cascade light-emitting-diodes and superluminescent-diodes at the 1.04- $\mu$m wavelength regime," in *Lasers and Electro Optics Society (LEOS) Meeting*, Newport Beach, CA, Nov. 2008, Paper WV 2.

[6] Y. Wang, J. S. Nelson, Z.-P. Chen, B. Reiser, R. Chuck, and R. Windeler, "Optimal wavelength for ultrahigh-resolution optical coherence tomography," *Opt. Express*, vol. 11, no. 12, pp. 1411–1417, Jun. 2003.

[7] F. Dross, F. van Dijk, and B. Vinter, "Optimization of large band-gap barriers for reducing leakage in bipolar cascade lasers," *IEEE J. Quantum Electron.*, vol. 40, no. 8, pp. 1003–1007, Aug. 2004.

[8] M. L. Osowski, R. M. Lammert, D. V. Forbes, D. E. Ackley, and J. J. Coleman, "Broadband emission from InGaAs–GaAs–AlGaAs LED with integrated absorber by selective-area MOCVD," *Electron. Lett.*, vol. 31, no. 17, pp. 1498–1499, Aug. 1995.

[9] C.-F. Lin, Y.-S. Su, C.-H. Wu, and G. S. Shmavonyan, "Influence of separate confinement heterostructure on emission bandwidth of InGaAsP superluminescent diodes/semiconductor optical amplifiers with nonidentical multiple quantum wells," *IEEE Photon. Technol. Lett.*, vol. 16, no. 6, pp. 1441–1443, Jun. 2004.

[10] L. A. Coldren and S. W. Corzine, *Diode Lasers and Photonic Integrated Circuits*. New York: Wiley, 1995, ch. 2.

[11] M. Sugo, Y. Shibata, H. Kamioka, M. Yamamoto, and Y. Tohmori, "High-power (>80 mW) and high-efficiency (>30%) 1.3 $\mu$m superluminescent diodes," *Electron. Lett.*, vol. 42, no. 21, pp. 1245–1246, Oct. 2006.